Formability Studies on Aluminum Alloy Sheets through Deep Drawing Process

U. Pranavi[1], P. Venkateshwar Reddy[2], Perumalla Janaki Ramulu[3#]

[1, 2]PG Scholar, Department of Mechanical Engineering, Vardhaman College of Engineering, Hyderbad-501218

[3]Department of Mechanical Engineering, Vardhaman College of Engineering, Hyderbad-501218

Abstract

In this paper, the effects of lubricating conditions and blank holding force on deep drawing process for understanding the formability of AA 6061 aluminum alloy sheet of 2 mm thickness is studied. The numerical simulations are performed for deep drawing of square cups at three different lubricating conditions and blank holding forces. For numerical simulation PAM STAMP 2G a commercial FEM code in which Hollomon's power law and Hills 1948 yield's criterion is used. Two different strain paths (150x150 and 200x200) were simulated. Punch forces and dome heights are evaluated for all six conditions. Failure initiation and propagation is also observed. From the overall results, it has been noted that by increasing the lubricating conditions and blank holding forces, punch forces and dome height variations are observed by which one can predict the formability for different strain paths.

Keywords: *deep drawing; process parameters; blank holder force; friction coefficient*

1 Introduction

Deep drawing is a manufacturing process that is used extensively in the forming of sheet metal into cup or box like structures under tensile and compressive conditions, without altering the sheet thickness. Pots and pans for cooking, containers, sinks, automobile parts, such as panels and gas tanks, are among a few of the applications manufactured by sheet metal deep drawing. The formability of a blank during the deep drawing is depends on the process parameters such as blank holder force, lubrication, punch and die radius, die–punch clearance, in addition to mechanical properties and thickness of the sheet metal and part's geometry. Many studies have been carried out on numerical simulations of deep drawing process. For example, Meinders *et al*. (2000) investigated the behavior of tailored blanks during deep drawing using the finite element code. They simulated the deep drawing of two products using Tailored Blanks and observed that the experimental and simulation results were correlated satisfactory. Takuda *et al*. (2002) simulated the deformation behavior and the temperature change in deep drawing of an aluminum alloy sheet and successfully predicted the forming limit and necking site by comparing the numerical results with experimental results. Yoshihara *et al* (2005) investigated deep-drawing process of a circular cup using magnesium alloy material and found that wall thickness of the drawn cup depends on the initial BHF value. Padmanabhan *et al* (2007) evaluated the orientation of blank sheets rolling direction during deep drawing process and the effect of anisotropy in the tailor-welded blank and noticed that the punch force for deep drawing increases with anisotropy in the blank sheets.

Jawad *et al*. (2008) studied the effects of varying punch nose radius used in the deep drawing process by carrying out the numerical simulation process in commercially finite element program code. Compared the experimental work with numerical results, it was concluded that large frictional force is applied to the metal by the edge of the punch, but not by its flat section. Also the work required to form a part with large nose radius is more than that required to form a part with small punch nose radius. Hama *et al*. (2008) studied the tool modeling accuracy on a square-cup

deep-drawing operation using finite element simulation and quadratic parametric surfaces proposed by Nagata patch. It was presented that the total number of tool elements can be reduced to about 10% of the polyhedral model. Rodrigues *et al*. (2009) determined a multi-step analysis for admissible blank-holder forces in deep drawing process for stamping friction stir welded tailored blanks and the formability behavior of similar and dissimilar combinations of AA 5182-H111 and AA 6016-T4 aluminum alloys were previewed. Using the theoretical stress based criteria; analytical FLDs were plotted and compared their formability limits with the principal strains in the cup walls obtained by the numerical simulation of the deep-drawing tests, thereby concluded that the procedure can be used to determine the maximum BHF for deep drawing different TWBs. Arab *et al* (2013) examined the deep drawing process of axisymmetric cylindrical cup with anisotropic Hill's non-yield criterion and rigid viscoplastic finite element method. The experimental validation of the numerical prediction was found to be satisfactory for thickness distributions and deformation stages on the sheet.

From the above studies, it is observed that the essentiality of the proper selection of process parameters to the deep drawing process is very crucial. The process parameters selection is also depends on the base material. It is essential to study the process numerically before experimentation. The objective of the present work is to identify the desired lubrication and blank holding force for AA 6061 alloy during the deep drawing process.

2 Methodology

2.1 Base material properties and process parameters

For conducting simulation, the material and process parameters that affect the deep drawing behavior were identified from available literature. The mechanical and forming properties of aluminum base metal used in FE simulations are shown in Table 1. The effectible parameters of deep drawing process parameters like coefficient of friction and blank holding force were considered for simulation. These two parameters were varied in three levels as shown in Table 2.

Table 1 Mechanical properties of base material AA 6061-T6 [Ramulu *et al.* (2013)]

Base	AA 6061-T6
E (GPa)	66
γ	0.33
σ (MPa)	269
K (MPa)	419
n	0.1
R_o	0.79
R_{45}	0.95
R_{90}	0.85
t (mm)	2

Table 2 Three levels Process parameters and considered value

Process parameters	Value
Coefficient of Friction (μ)	0.1 0.15 0.2
Blank holding force (BHF) (kN)	10 20 15

2.2 Modeling and Simulation of Deep drawing process

In CAD modeling, the tools required for the test, blank, punch, blank holder and die were generated as shown in Figure 1. Simulations of deep drawing process were simulated using a finite element code. The sheet comprised of quadrilateral shell elements with five through thickness integration points of Belytschko-Tsay formulation. The strain hardening law and the plasticity model considered were the Hollomon's power law ($\sigma = K\varepsilon^n$; where σ-true yield strength; K-strength coefficient; ε-true strain; n-strain hardening coefficient) and the Hill's 1948 isotropic hardening yield criterion respectively. Two base material sheets each of size 150x150mm and 200x200mm were taken for all the conditions. A uniform meshing of size 1mm was used throughout the simulations. The yield strength was kept constant and the friction coefficients taken were 0.1, 0.15 and 0.2. The blank holder forces considered were 10kN, 15kN and 20kN. Downward stroke to the punch is given with a velocity of 10mm/min and a total of 18 simulations were performed by varying the coefficient friction and blank holder force. From the simulation results the thickness distribution, punch force, and dome height were evaluated.

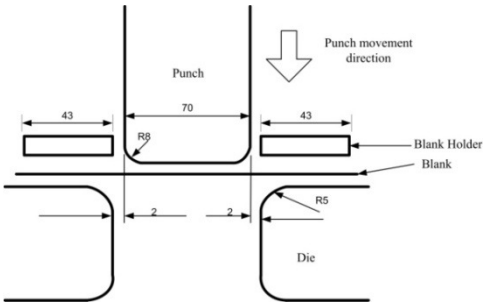

Figure 1 Deep drawing set for simulations

3 Results and Discussion

The formability of a blank sheet depends on the process parameters such as blank holder force, lubrication, punch and die radius, die–punch clearance, in addition to mechanical properties and thickness of the sheet metal and part's geometry. Among these parameters, blank holding force and lubrication are varied in three levels and simulated whole process. From the simulation results, punch force and thickness distribution are compared in the followed sections for evaluating the effectiveness of blank holding force and lubrication on AA 6061 sheets during deep drawing process.

3.1 Punch force evolution

Figure 2 shows punch force comparison of 150x150 mm strain path at different blank holding forces (10, 15 and 20 kN) at same lubricating condition (0.1). It is observed that by increasing the blank holding force from 10kN to 20kN punch force variation is not much, but it increased slightly as shown in Table 3. In the similar manner, it has seen for other conditions also as shown in Fig. 3 and 4. In these conditions also punch force is increased by increasing the blank holding force without changing lubrication condition for the 150x150 mm strain path.

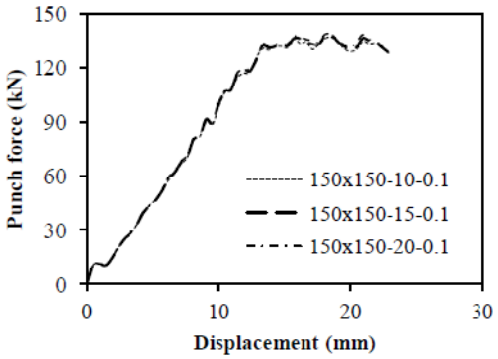

Figure 2 Punch force comparison at different blank holding forces at same lubricating condition (0.1)

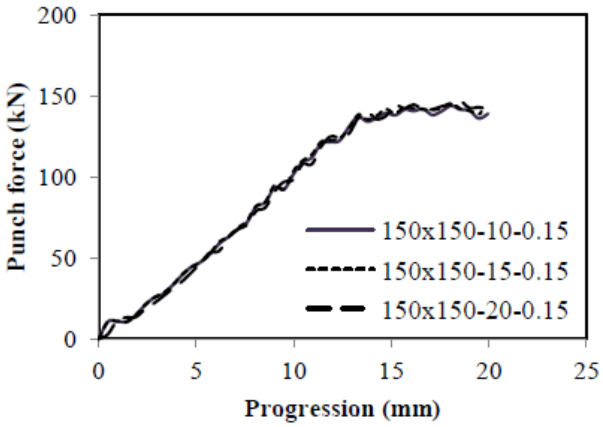

Figure 3 Punch force comparison at constant frictional coefficient (0.15) and at different blank holding forces

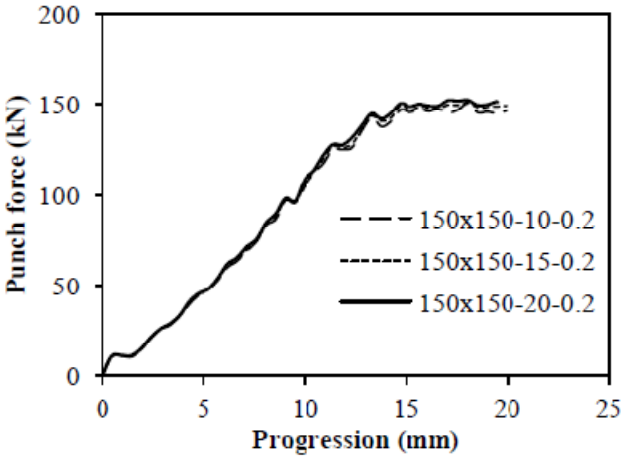

Figure 4 Punch force comparison at constant frictional coefficient (0.2) and at different blanks holding forces

Figure 5 shows punch force comparison analysis of 200x200 mm strain path at three different blank holding forces (10, 15 and 20 kN) at same lubricating condition (0.1). It is observed that by increasing the blank holding force from 10kN to 20kN punch force is decreased as shown in Table 3, but the variation is very less. For blank holding forces 15kN and 20kN punch force is almost the same. In the similar manner, it has seen for other conditions also as shown in Fig. 6 and 7. In these conditions also punch force is decreased by increasing the blank holding force.

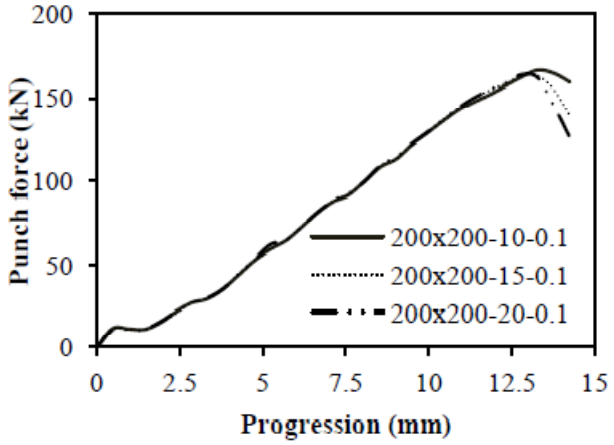

Figure 5 Punch force comparison at constant friction coefficient (0.1) and at different blank holding forces

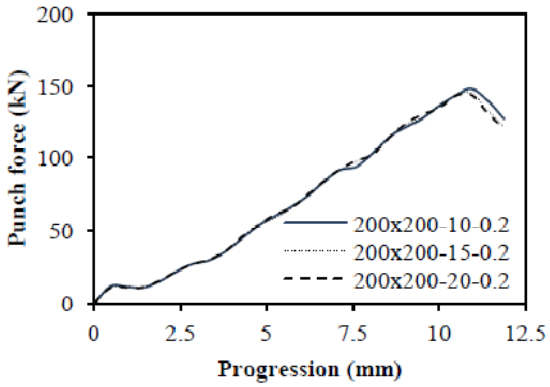

Figure 6 Punch force comparison at constant frictional coefficient (0.2) and at different blanks holding forces

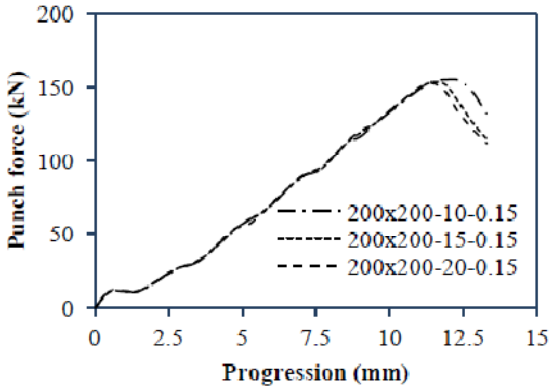

Figure 7 Punch force comparison at constant frictional coefficient (0.15) and at different blanks holding forces

Table 3 Maximum punch force at different condition

Strain path	Lubrication Condition	Blank holder force (kN)	Maximum punch force (kN)
150x150 mm	0.1	10	136.9
		15	138.2
		20	138.4
	0.15	10	143.8
		15	145.3
		20	146.6
	0.2	10	150.8
		15	151.5
		20	152.5
200x200 mm	0.1	10	166.5
		15	163.5
		20	163.9
	0.15	10	155.3
		15	153.5
		20	150.1
	0.2	10	147.8
		15	145.1
		20	143.8

3.2 Failure location and Dome height

In all the simulations, failure initiation is observed at the side walls of the blanks as shown Fig. 8 (a) & (b) and failure propagation has happened around the side walls as shown Fig. 8 (c). The dome height at which the blank takes the initial necking corresponding progression is treated as dome height. The necking is based on the thickness gradient necking criterion (Nandedkar, (2000)). According to this criterion the ratio of two consequents elements should be less than or equal to 0.92 as shown in below equation

$R_{\text{thickness gradient}} = R_c = \frac{tn}{tn-1} \leq 0.92$ => material failure or necking

For the all the simulation conditions, dome height (progression at which 0.92 has obtained) and initial failure progression state has mentioned in the Table 4. It is observed that dome height is more when lubrication condition is at 0.1 and decreased correspondingly irrespective of the blank holding force and strain paths.

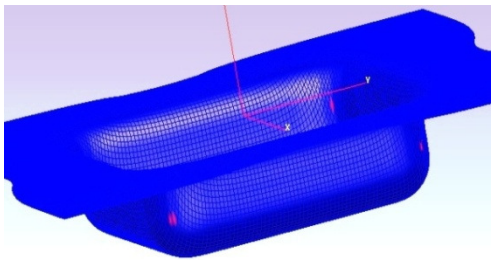

(a) Failure initiation in 150x150 mm strain path

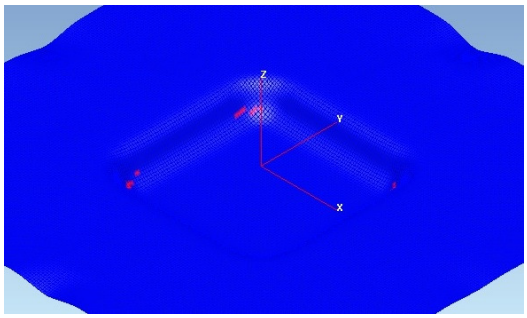

(b) Failure initiation in 200x200 mm strain path

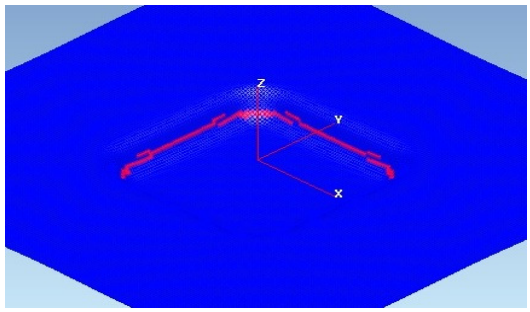

(c) Failure propagation in 200x200 mm strain path strain path

Figure 8 Failure initiation and propagation during the simulation

Table 4 Dome height and initial failure progression state

S. No	Condition	Dome Height (mm) (based on TGNC)	Initial failure location Progression (mm)
1	150x150-10kN-0.10	23.0	18.52
2	150x150-10kN-0.20	14.0	18.05
3	150x150-10kN-0.15	18.0	18.05
4	150x150-15kN-0.10	18.0	18.53
5	150x150-15kN-0.20	14.0	18.05
6	150x150-15kN-0.15	16.0	18.05
7	150x150-20kN-0.10	18.0	18.05
8	150x150-20kN-0.20	13.0	18.05
9	150x150-20kN-0.15	18.0	18.52
10	200x200-10kN-0.10	13.0	13.30
11	200x200-10kN-0.20	11.0	10.92
12	200x200-10kN-0.15	12.0	11.87
13	200x200-15kN-0.10	13.0	12.82
14	200x200-15kN-0.20	11.0	10.92
15	200x200-15kN-0.15	12.0	11.40
16	200x200-20kN-0.10	13.0	12.82
17	200x200-20kN-0.20	11.0	10.92
18	200x200-20kN-0.15	12.0	11.40

4 Conclusions

From the deep drawing formability study on AA 6061 alloy, the effect of blank holding forces and lubricating conditions on the punch force and dome height variations are evaluated. The following conclusions are drawn.

1. The effect of lubrication on the punch force during the simulation is noted as by increasing the coefficient of friction punch force is improved for 150x150 mm strain path whereas it is reverse for 200x200 mm strain path. Similar behavior is seen with the blank holding force for both the strain paths.

2. The failure initiation in the strain paths of 150x150 and 200x200 mm are same irrespective of the changed parameters during simulation process.

3. Dome height is maximum (23 mm) for the condition of μ=0.1 and BHF=10kN for 150x150mm strain path whereas minimum (11 mm) is observed in the 200x200mm strain path. Overall, when the punch force is less dome height is maximum and vice versa.

References

Meinders, T., Vanden Berg, A., and Huetink, J. (2000), Deep drawing simulations of tailored blanks and experimental verification, *Journal of Materials Processing Technology,* 103, pp. 65-73.

Takuda, H., Mori, K., Masuda, I., Abe, Y., Matsuo, M. (2002), Finite element simulation of warm deep drawing of aluminum alloy sheet when accounting for heat conduction, *Journal of Materials Processing Technology,* 120, pp. 412–418.

Yoshihara, S., Ken-ichi Manabe, Hisashi Nishimura, (2005), Effect of blank holder force control in deep drawing process of magnesium alloy sheet, *Journal of Materials Processing Technology,* 170, pp. 579–585.

Padmanabhan, R., Baptista, A. J., Oliveira, M. C., Menezes, L. F. (2007), Effect of anisotropy on the deep-drawing of mild steel and dual-phase steel tailor-welded blanks, *Journal of Materials Processing Technology*, 184, pp. 288–293.

Waleed K. Jawad, Jamal H. Mohamed, (2008), Studying the effect of punch nose radius on deep drawing operation, *Eng. And Tech*., 26, pp. 55-73.

Takayuki Hama, Masato Takamura, Akitake Makinouchi, Cristian Teodosiu and Hirohiko, (2008), Effect of Tool-Modeling Accuracy on Square-Cup Deep Drawing Simulation, *Materials Transactions*, 49, pp. 278 - 283.

Rodrigues, D. M., Leitao, C., Menezes, L. F., (2010), A Multi-Step Analysis for Determining Admissible Blank-Holder Forces in Deep-Drawing Operations, *Materials and Design*, 31, pp. 1475-1484.

Najmeddin Arab (2013), Experimental and Cylindrical Simulation Analysis of Deep Cylindrical Simulation Analysis of Deep Cylindrical Cup Process, *Merit Research Journal of Petroleum, Geology and Minimg*, 1(1), pp. 001-008.

Janaki Ramulu, P., Ganesh Narayanan, R., Kailas, S. V., Jayachandra Reddy, 2013. "Internal defect and process parameter analysis during friction stir welding of Al 6061 sheets". *International Journal of Advanced Manufacturing Technology*, 65, pp. 1515-1528.

Nandedkar, V. M. (2000), Formability studies on a deep drawing quality steel, *PhD Thesis.* IIT Bombay, India.